Optical Fiber Technology 75 (2023) 103209

Contents lists available at ScienceDirect

Optical Fiber Technology

journal homepage: www.elsevier.com/locate/yofte

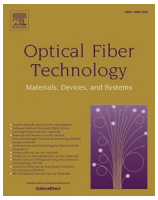

Fabrication and characterization of active polymer optical fibers with a ring-doped structure

Igor Ayesta [a,*], Mikel Azkune [b], María Asunción Illarramendi [c], Eneko Arrospide [a], Joseba Zubia [d], Gaizka Durana [d]

[a] Department of Applied Mathematics, Engineering School of Bilbao, University of the Basque Country (UPV/EHU), Torres Quevedo 1, 48013 Bilbao, Spain
[b] Department of Electronic Technology, Engineering School of Bilbao, University of the Basque Country (UPV/EHU), Torres Quevedo 1, 48013 Bilbao, Spain
[c] Department of Applied Physics, Engineering School of Bilbao, University of the Basque Country (UPV/EHU), Torres Quevedo 1, 48013 Bilbao, Spain
[d] Department of Communications Engineering, Engineering School of Bilbao, University of the Basque Country (UPV/EHU), Torres Quevedo 1, 48013 Bilbao, Spain

ARTICLE INFO

Keywords:
Polymer optical fibers
Luminescent materials
Ring-doped structure
Fiber lasers and amplifiers
Tunable light-sources
Optical fiber based sensors
Solution-doping technique

ABSTRACT

This paper employs the solution-doping technique for the fabrication of polymer optical fibers (POFs) doped with two perylene derivatives, Lumogen Yellow 083 and Lumogen Red 305, in different combinations. With the solution-doping technique is very easy to control the amount of dopant penetration into the core of non-doped uncladded fibers, allowing the fabrication of active POFs with a novel ring-doped structure. In addition to manufacturing the fibers, these have also been optically characterized. Specifically, the influence of the combination of dopants, pumping power and wavelength, as well as the light propagation distance, have been measured and analyzed. Furthermore, time-resolved emission characteristics have also been measured to determine the fluorescence lifetimes and to extract information about the energy transfer between the dopants. Finally, the aim of this work has been to investigate the performance of the aforementioned POFs for fluorescent lighting applications, with a special focus on tunable light sources, and also for sensing applications.

1. Introduction

In recent years, interest in the field of photonics has grown due to the incorporation of functional materials into solid-state organic hosts, such as polymer optical fibers (POFs) [1]. This kind of fibers are preferable to silica optical fibers because they are easier and more economical to manufacture, safer to handle and much more flexible [2,3]. In addition, the manufacturing temperature of POFs is much lower than that of glass fibers, allowing a wide range of dopants to be embedded in the fiber core, from organic dyes and conjugated polymers to other types of materials such as rare-earth ions and quantum dots [4–6]. The emission and absorption characteristics of these dopants are suitable for achieving luminescence in the visible region of the spectrum, just in the low-attenuation windows of POFs, which is of interest for a wide range of applications. For example, for the development of optical sensors [7,8], for luminescent solar concentrators [9,10], and for luminescent speckle-free light sources [11,12].

There are different options to incorporate the dopant molecules into the Poly(methyl methacrylate) (PMMA) core of POFs. Usually, the doping process is carried out during the fabrication of POF preforms, in which the dopant molecules are added to the monomer mixture before the polymerization process takes place [13,14]. Then, the preforms are heated to above the glass transition temperature of PMMA and drawn into fibers of required diameters using the thermal fiber-drawing technique. However, its main disadvantage is that expensive fiber-drawing towers are needed for that purpose. In addition, a great deal of know-how of their use is required to obtain doped POFs with the desired physical and optical parameters, which can take a long time to learn [15]. Alternatively, the dopant molecules and the melted PMMA can be mixed in the extrusion line of co-extrusion manufacturing technique [16]. Co-extrusion provides a scalable way to prepare graded-index or micro-structured fibers [17,18], but the costly and complicated equipment limits its applicability. Wet-spinning is another technique for manufacturing doped POFs, in which the polymer host, mixed with the desired dopant molecules, is dissolved at mild temperatures, and then it is spun into the coagulation bath and drawn into a fiber [19,20]. This technique requires less technical equipment than the previous ones but the formation of exact fiber cross section is difficult to control because of

* Corresponding author.
E-mail address: igor.ayesta@ehu.eus (I. Ayesta).

https://doi.org/10.1016/j.yofte.2022.103209
Received 4 October 2022; Received in revised form 23 November 2022; Accepted 18 December 2022
Available online 24 December 2022

inward and outward mass transfer process. An alternative technique to incorporate dopant molecules into the core material is the so-called solution-doping technique, in which the process is carried out directly in the optical fiber [21,22]. Briefly, the desired dopant molecules are mixed with a non-solvent of PMMA, usually with methanol, and POFs are immersed into the solution. Then, POFs are swollen by the non-solvent and dopant molecules diffuse into the core material. The technique has already been used to incorporate Rhodamine 6G, Rhodamine B or *trans*-4-stilbenemethanol into ad-hoc, commercial step-index and also micro-structured POFs [22–25]. The doping process is easy to undertake and low-cost, as there is no need to use any kind of drawing tower or equipment. This procedure also opens up the opportunity for any research group to manufacture their own ad-hoc doped POFs for any specific application requiring particular characteristics, such as distinct dopant molecules or fiber diameters. Another advantage that makes this technique interesting is that it is possible to dope only one end of the fibers, transforming it into an active part. That makes fibers that are both active and passive at the same time, without the need to connect fibers of different nature, thus avoiding coupling losses between them. Although there are some authors investigating how to optimize this technique, e.g. by using binary non-solvent/solvent mixtures or aqueous solutions at elevated temperatures [23,25], there is still some recent work where only the cladding material could be doped, due to the barrier formed by the core/cladding interface. However, following the procedure described in this paper, we have obtained POFs with a partially doped core, forming a ring-doped structure. This type of ring structure, together with the incorporation of two perylene derivatives (Lumogen Yellow 083 and Lumogen Red 305), make it possible to obtain interesting emission features, which can be very attractive not only for the development of light sources with tuning characteristics but also for sensing applications. As far as we know, this is the first time that such doped POFs and their optical characterization have been reported.

The paper is organized as follows. First, the method for preparing the samples is explained. Then, the different experimental setup employed in this work are described. Finally, the optical characterizations of both the solutions and the doped POFs are shown and discussed.

2. Materials and methods

2.1. Sample preparation

The POF samples employed in this work were fabricated by our research group from Plexiglass® extrusion rods purchased from Evonik. These were 20 mm in diameter and were annealed in a C-70/200 climate chamber (Controltecnia-CTS) for 7 days at a temperature of 90 °C under low relative humidity. Afterwards, they were drawn into only–core fibers of 500 μm in diameter, with an accuracy of ± 1 %, using our own POF drawing tower [26]. The refractive-index profile of the fibers was step-index in all cases.

To incorporate Lumogen (BASF) dopant molecules into the pristine only core fibers, samples of around 15 cm in length were cut and put into an oven at a temperature of 60 °C in order to eliminate any possible residual stress. Two main solutions were made, one consisting of Lumogen Yellow 083 and methanol (LY10LR0), and another consisting of Lumogen Red 305 and methanol (LY0LR10). In each case, the concentration was 0.025 w/v. Then, they were mixed in different percentages, to obtain new solutions: LY9LR1, LY8LR2, LY7LR3, LY6LR4, LY5LR5, LY4LR6, LY3LR7, LY2LR8 and LY1LR9. The reason for utilizing methanol as solvent is that Lumogen can be easily solved in it, but not the PMMA, preventing the formation of dopant aggregates, which has detrimental effects on the light-emission features of doped fibers [6]. Moreover, methanol is less aggressive with PMMA material than other solvents, and as it is quite volatile, it can be removed from the PMMA at room temperature [24]. Several laboratory test tubes were filled with the different solutions and fiber samples were placed in each tube and stored at room temperature. After the desired time, the fibers were taken out of the solutions, thoroughly rinsed and dried at room temperature. Then, a close look at the cross-sections of these samples through an optical microscope allowed us to ensure the desired lateral penetration. Finally, each sample was cut at a distance of around 3 mm from one of its ends, which was polished by hand using polishing paper and connectorized with SMA connectors.

2.2. Experimental set-ups

Three different experimental setups were employed in this work. The first one was used to measure the absorption spectra of the different Lumogen-methanol solutions and of the doped fibers and also to acquire the emission spectra of the solutions. The emissions of the doped fibers, were obtained using the second setup, in which the side illumination technique was employed. Finally, the third setup was used to obtain time-resolved emission spectra of the fibers.

Fig. 1 shows the experimental setup employed to measure the absorption of the Lumogen-methanol solutions and of the doped fibers. An AvaLight-DH-S-BAL BALANCED POWER (Avantes) was used as light source and its emission was guided along a 1 m long fiber (core diameter of 200 μm) up to a CUV-ALL-UV/VIS Cuvette Sample Holder (Avantes) where each sample was placed during the measurement. The light that went through the sample was collected by another 1 m long fiber, 600 μm in diameter, and it was finally guided to an AvaSpec-ULS2048CL-EVO-RS-UA spectrometer (Avantes). A white-reference measurement with an empty cuvette was taken to calculate the absorbance of each sample. In order to measure the absorbance of the solution or doped POFs, both the illumination and reception fibers were facing each other along a straight line. Besides, an ad-hoc POF holder was built to ensure the correct illumination of the fiber samples using the same cuvette holder. For the case of the fluorescence emission for the solutions, the reception fiber was aligned perpendicularly to the illumination fiber to measure the fluorescence emission from the solution and to remove any remaining emission from the source.

Fig. 2 sketches the experimental setup employed for light emission spectra measurements by means of the side-illumination technique [27,28]. The POF sample was excited laterally and the light emitted from the excitation point propagated along the fiber sample over a distance that could be adjusted by moving an ILS250CC (Newport) linear stage driven by an ESP300 (Newport) motion controller. In all the measurements carried out using the side-illumination technique, the emitted light always propagated through a non-excited fiber length of 3.5 cm before reaching the spectrometer (due to the length of the SMA connector at the fiber end). The light was finally collected by an USB4000-UV–vis spectrometer (Ocean Optics) placed at the end of the sample, with an optical resolution of 1.5 nm for the full width at half-maximum (FWHM). The excitation light source was a Mai Tai HP laser system (Newport), which emits Gaussian light pulses of around 100 fs width at a repetition rate of 80 MHz in a spectral emission range between 690 and 1040 nm, with peak powers of 300 kW and an average power of 2.5 W. The spot of the laser beam was 1.2 mm in diameter. In order to be able to excite from 345 nm to 520 nm, the wavelength of the original light was downshifted by using a second harmonic generator (Inspire Blue). The excitation irradiance was controlled by placing a variable attenuator after the laser output. The whole acquisition system was automated by means of an ad-hoc LabVIEW program.

Lastly, Fig. 3, which is a variant of the previous one, shows the experimental setup used to obtain time-resolved emission spectra of the doped fibers. A Spectra Physics 3986 pulse picker (Newport) was introduced in the excitation part of the setup to reduce the repetition rate of the Mai Tai HP laser system to 8 MHz, and the whole acquisition system from Fig. 2 was replaced by a combination of the Acton SP2300 monochromator (Princeton instruments) and the C10627 ultrafast Streak Camera (Hamamatsu). This combination provided the option to resolve the acquired signals both spectrally and temporally, which means that the whole spectrum was obtained at the same instant of time.

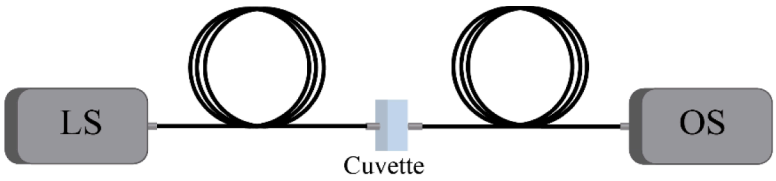

Fig. 1. Experimental setup employed to measure the absorption of the Lumogen-methanol solutions and of the doped fibers, and the emission spectra of the solutions. LS: light source, OS: optical spectrometer.

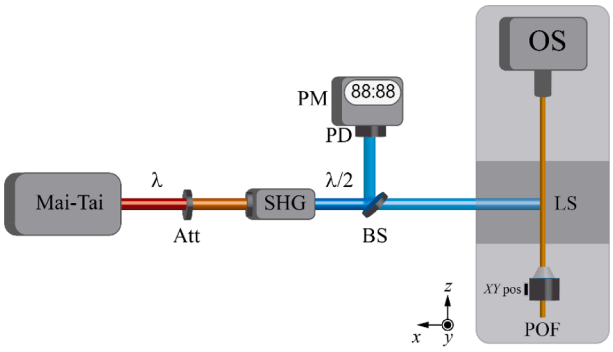

Fig. 2. Experimental setup employed to measure the emission spectra of doped POFs by means of the side-illumination technique. Att: variable attenuator; SHG: Inspire Blue second harmonic generator; BS: beam splitter; PD: photodetector; PM: power meter; LS: linear stage; xy-POS: xy-micropositioner; OS: optical spectrometer.

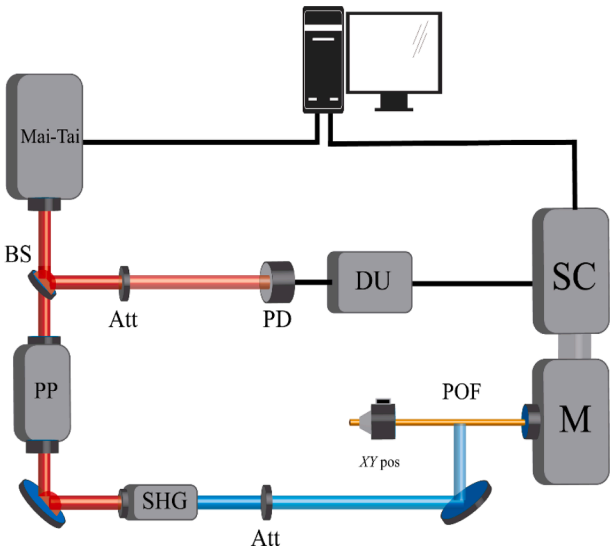

Fig. 3. Experimental set-up employed to carry out the time-resolved measurements. BS: beam splitter; Att: variable attenuator; PD: photodetector; DU: delay unit; PP: pulse picker; SHG: second-harmonic generator; xy-POS: xy-micropositioner; POF: polymer optical fiber; M: monochromator; SC: Streak Camera.

In order to properly synchronize both the excitation and the acquisition systems, a small amount of the laser signal was split from the laser output and directed to a photodetector, whose electric signal was delayed by means of a delay unit. A precise use of this delay unit guaranteed the visualization of the transmitted pulses on the corresponding temporal window of the Streak Camera. The Hamamatsu HPDTA software controlled both parts of the system. Once the acquisition was performed, the data analysis was carried out by employing an ad-hoc Matlab program.

3. Results

3.1. Experimental results on solutions

In order to know the optical features of the employed Lumogen dopants, i.e. Lumogen Yellow and Lumogen Red, first of all, the absorption and emission spectra corresponding to each dopant solution were measured. The results are depicted in Fig. 4. For the Lumogen Yellow, the main absorption bands are centered at 475 nm and at 445 nm, and the emission band presents its maximum at 490 nm. On the other hand, in the case of Lumogen Red, it presents a maximum absorption at 575 nm and a secondary absorption band with a peak at 445 nm. Additionally, the emission band has its maximum at 630 nm. These absorption and emission values are in good agreement with those previously reported [5]. The choice of these two dopants is interesting because they present smaller overlap between the absorption and emission bands than other organics dyes, such as Rhodamine dyes, which has beneficial effects in the reduction of losses due to reabsorption and reemission effects. Moreover, the emission band of Lumogen Yellow overlaps significantly with the main absorption band of Lumogen Red, which enables the energy transfer effect between them. In that case, Lumogen Yellow plays the donor role and Lumogen Red the receptor role, for a correct band-to-band transition [29].

Afterwards, the absorption and emission spectra of the eleven solutions of Lumogen and methanol were measured. The obtained results are displayed in Fig. 5 and in Fig. 6, respectively. As expected, the absorption spectra evolve progressively from the pure Lumogen Yellow absorption band to the Lumogen Red band as the latter's concentration increases. The maximum absorbance value is achieved with LY0LR10 sample, at 575 nm. The emission spectra evolve in a similar way. That is, the emission band corresponding to Lumogen Yellow decreases in intensity whereas the emission band of the Lumogen Red becomes more noticeable. However, it is noteworthy that the maximum emission value obtained for the Lumogen Red emission band is not achieved for the LY0LR10 case but for the LY6LR4. That is a consequence of the energy transfer effect between the dopants, in which the emission band corresponding to the Lumogen Red is enhanced due to energy provided by the donor Lumogen Yellow.

3.2. Experimental results on POFs

Once the absorption and emission spectra of the eleven solutions consisting of Lumogen dyes and methanol were measured, 15 cm long pristine POFs were introduced in each solution. As an example, the left side of Fig. 7 shows cross-sectional images of samples that were previously immersed in LY10LR0, LY5LR5 and LY0LR10, at room temperature for 7 h, achieving a dopant penetration of 35 %. That is, the outer ring-like area representing 35 % of the core cross-sectional area, was doped whereas the rest remained unchanged. The lateral penetration depth of the solution is clearly visible, because of the clear boundary between the outer ring, with different color depending on the employed solution, and the intact transparent inner region. The top three images were obtained with a microscope when the doped POFs where excited with white light in transmission mode, whereas the bottom three images were obtained by exciting the POF samples with a UV lamp in reflection

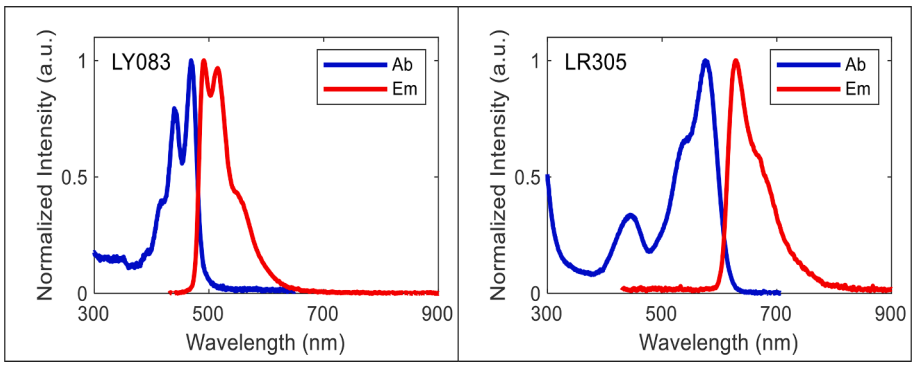

Fig. 4. Normalized absorption (blue line) and emission (red line) spectra of solutions of (left) Lumogen Yellow and methanol, and (right) of Lumogen Red and methanol.

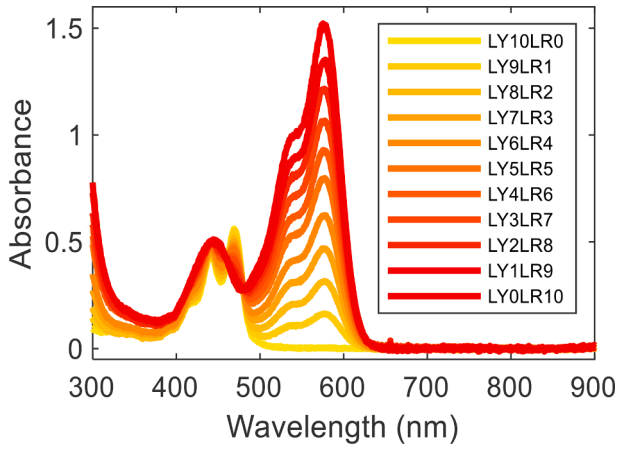

Fig. 5. Absorption spectra of methanol solutions of Lumogen Yellow and/or Lumogen Red.

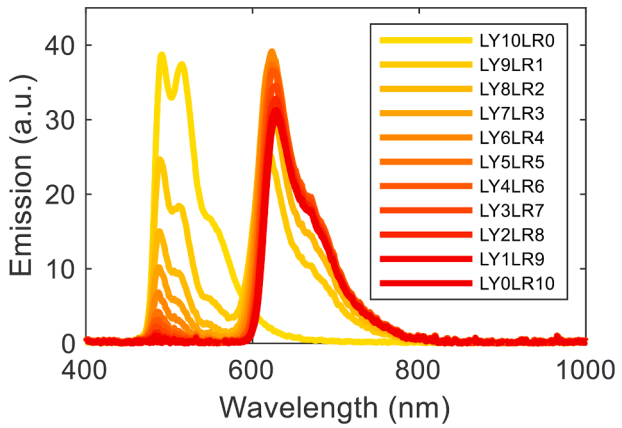

Fig. 6. Emission spectra of methanol solutions of Lumogen Yellow and/or Lumogen Red.

mode.

As previously mentioned, one of the advantages of this doping technique is the ease of controlling the amount of dopant penetration, which makes it possible to create doped POFs with ring structures [22]. Later on, it will be shown how this type of structures provide very interesting optical properties for the development of broadband light sources and for sensing applications. In addition, this doping technique allows doping only one end of the pristine fiber, transforming it into an active part, as can be seen on the right-hand side of Fig. 7. This makes it possible to create fibers that are both active and passive at the same time, without the need to connect fibers of different nature, thus avoiding coupling losses between them. These features, to date, have not been possible to create using more common techniques, such as the use of fiber-drawing towers.

Samples of 1 cm in length were cut from each doped POF and carefully polished with polishing papers to measure their absorbance. As commented in "Experimental-setups" section, a 3D-printed ad-hoc POF holder was used for this purpose. Fig. 8 shows the obtained spectra for all POF samples. The PMMA absorption bands of the fibers appear clearly around 900 nm and on the UV side of the spectrum [30]. If these results are compared with those of Fig. 5, it can be seen that the absorption bands corresponding to Lumogen Yellow and to Lumogen Red are not affected by the polymer matrix. That is to say, there are no spectral shifts, but the dynamics observed in solutions change completely. Regardless of the amount of Lumogen Red used, the absorption band corresponding to the Lumogen Yellow, from 400 nm to 500 nm, absorbs the most. Moreover, the significant increase in the 500–600 nm band observed with solutions, as the amount of Lumogen Red is increased, is not observed in the case of doped POFs. That could be directly related to different penetration dynamics of the dopants during the diffusion process, since the molecular size of both dopants is different, being larger in the case of Lumogen Red [5]. That would make it more difficult for the latter to penetrate though PMMA than the former. Therefore, this effect should be taken into account when designing and fabricating active POFs if the solution-doping technique with multiple dopants is going to be used.

In contrast to the emission curves obtained from the solutions, where a white light source was used for the excitation, the emissions from the doped fibers were obtained with a pulsed laser (see Fig. 2). The fibers were laterally excited with an average light power of 11mW, which is well below the limit that would produce damages in the fibers. Both 445 nm and 475 nm were the excitation wavelengths considered, since they coincide with the two relative absorption maxima corresponding to Lumogen Yellow. In addition, 445 nm also coincides with the second absorption maximum of Lumogen Red. Fig. 9 shows that the maximum intensity is achieved with the sample doped only with Lumogen Yellow (LY10LR0), and the intensity obtained decreases as the concentration of this dopant decreases. In addition, as the concentration of the Lumogen Red increases, its corresponding emission band appears. However, this emission band does not grow continuously as a function of dopant concentration. It saturates and reaches the maximum value when the concentrations of both dopants are equal (LY5LR5), and then starts to decrease as the concentration of the Lumogen Red continues growing.

The obtained tendency in the emission spectra can be used advantageously to obtain the desired luminescence color, a feature especially interesting for designing and manufacturing light sources. From these emission spectra CIE 1931 chromaticity coordinates were calculated and presented in Fig. 10. The presented results show luminescence color

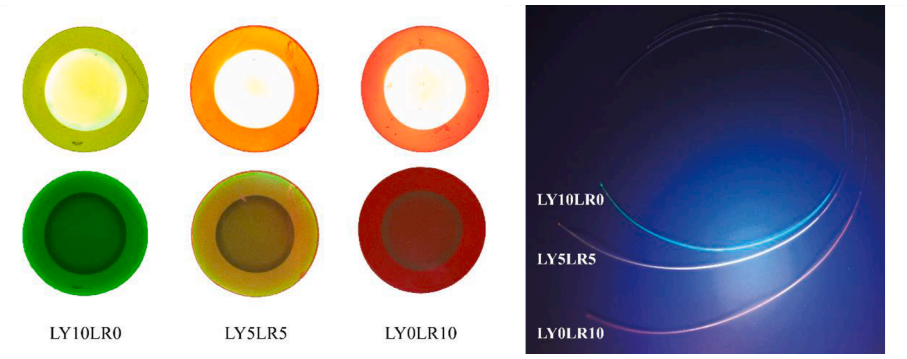

Fig. 7. Left side: microscope images of the cross-sections of POF samples immersed in three different solutions of Lumogen and methanol at room temperature for 7 h, namely (from left to right) LY10LR0, LY5LR5 and LY0LR10. The top images were obtained exciting the POF samples with white light in transmission mode, and the bottom ones by exciting then with a UV lamp in reflection mode. Right side: Fiber samples laterally excited with a UV lamp, where only one end of the fibers was doped while the other end remained unchanged.

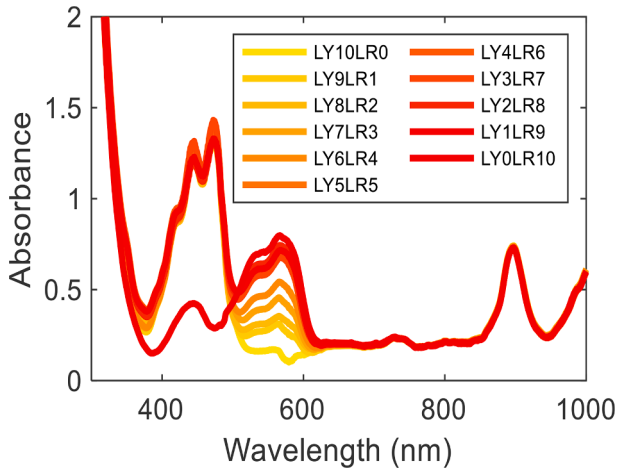

Fig. 8. Absorption spectra corresponding to the POF samples doped with Lumogen Yellow and/or Lumogen Red by using the solution-doping technique at room temperature for 7 h.

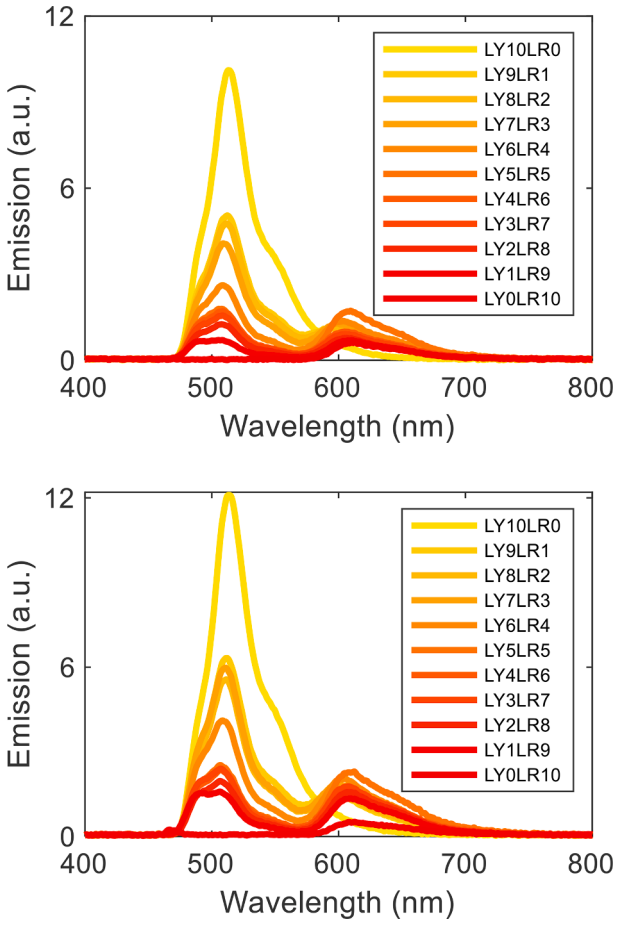

Fig. 9. Emission spectra corresponding to our POFs doped with Lumogen Yellow and/or Lumogen Red excited at 445 nm (up) and at 475 nm (down) using the side-illumination technique.

modification from green, through amber to red. In addition, it is worth mentioning that the addition of a third dopant to these fibers, especially to the LY5LR5 sample, would cause these coordinates to be blue-shifted, allowing white light fluorescence emission to be generated. This type of emission in POFs is very interesting for making light sources, sensing devices, and communications, among other [31–33].

Fig. 9 also shows that doping POFs only with Lumogen Red, i.e. LY0LR10 sample, is an inefficient option to obtain maximum intensity in the red region of the spectrum, since, as with solutions, the combination of dopants is more advantageous. Specifically, the LY5LR5 sample is the one with which the highest intensity is achieved in that spectral region, regardless of whether it is excited at 445 nm or 475 nm. One might think that the lower intensity at the output of the LY0LR10 sample is due to the fact that it was not optimally excited, i.e. at that wavelength where the absorption maximum of the Lumogen Red is located. However, if the same fiber is excited at 520 nm, which is the excitation wavelength value closest to the absorption maximum that our tunable laser allows –keeping the pumping power at 11 mW-, the signal in the red part of the spectrum is 50 % and 60 % lower than those obtained when exciting the samples at 445 nm and at 475 nm, respectively (see Fig. 11). Therefore, when manufacturing light sources based on doped POFs, it may be more interesting and efficient to use two dopants together instead of a single one. Nevertheless, this would require an appropriate choice of dopants to be used in each case. Furthermore, POFs doped with both dopants show two clearly differentiated emission bands, the first one corresponding to the emission band of the Lumogen Yellow -from 460 nm to 570 nm-, and the second one corresponding to the Lumogen Red -from 570 nm to 800 nm. This fact makes it possible, depending on the application, to work with each of these bands individually in a very simple way, by using optical filters, or with both bands simultaneously, which provides a great versatility to the light source.

Another interesting behavior was observed by varying the pumping power. The curves shown on top side of Fig. 12 represents the emission spectra of the LY5LR5 sample when the pumping power was increased from 11mW to 231mW, keeping the rest of parameters constant. It can be observed that increasing the power causes an increase in the intensity at the output of the LY5LR5 sample, as expected. However, the emission intensity increases more rapidly in the range corresponding to Lumogen Red. This behavior could suggest that the energy transfer from Lumogen Yellow to Lumogen Red is enhanced by increasing the pumping power. In addition, the bottom side of Fig. 12 shows the ratio between the

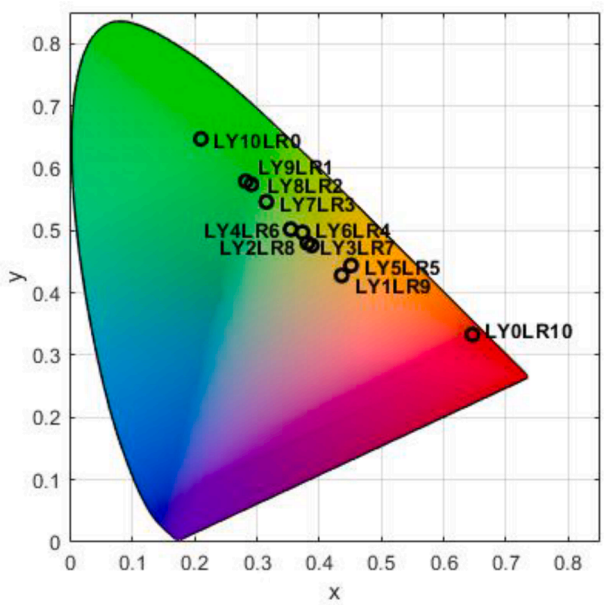

Fig. 10. The CIE 1931 chromaticity coordinates of our POFs doped with Lumogen Yellow and/or Lumogen Red excited at 445 nm using the side-illumination technique.

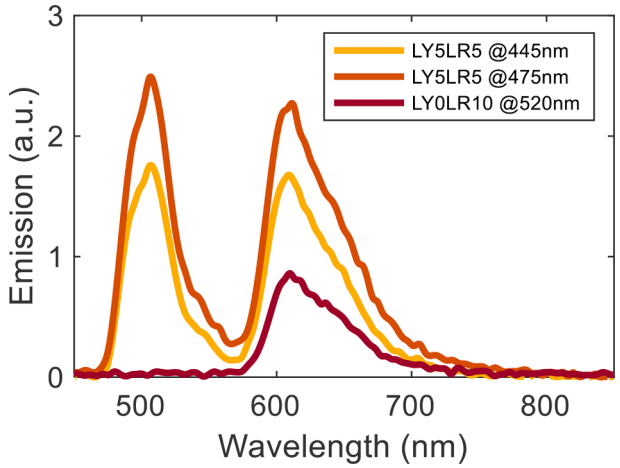

Fig. 11. Emission spectra corresponding to the sample LY5LR5 excited at 445 nm and at 475 nm, and to the sample LY0LR10 excited at 520 nm. In all cases, an excitation pump power of 11mW and the side-illumination technique were employed.

maximum emission intensity corresponding to Lumogen Red and the maximum emission intensity corresponding to Lumogen Yellow, measured at 609 nm and at 507 nm, respectively. The ratio as a function of pumping power is clearly linear, with a coefficient of determination of 0.999. This implies that, for the power range employed, no saturation effects are observed in the energy transfer between the dopants. Although higher powers could lead to higher ratio values or even yield some kind of saturation effect, they could cause irreparable physical damages to the POF samples. Nevertheless, within the power range considered, the observed effects may be of relevance when using these doped fibers as light sources, as they allow modifying the intensity of the red emission band with respect to the other emission band in a very controlled way and without the need for sample manipulation or replacement. On the other hand, the observed linear behavior suggests that variations in the power of the excitation source can be accurately determined by observing the ratio between both emission bands, making

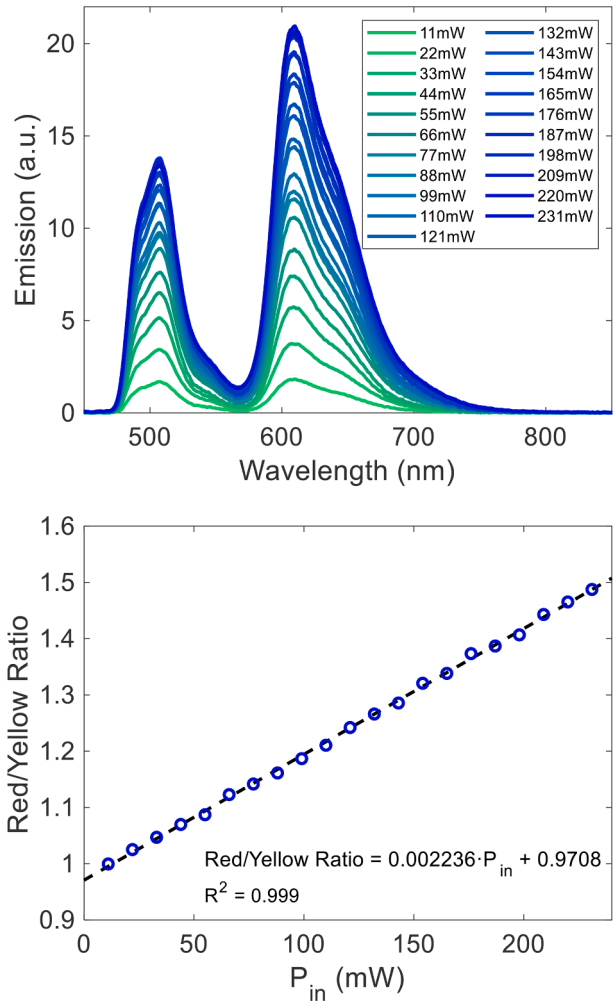

Fig. 12. Top side: Emission spectra corresponding to sample LY5LR5 excited with different powers at 445 nm. Bottom side: Ratio between maximum emission intensities of Lumogen Red (at 609 nm) and Lumogen Yellow (at 507 nm) as a function of the pumping power.

it possible to use these doped POFs also as sensors of the variation on the optical power of the excitation source.

Another interesting emission feature was observed analyzing the evolution of the emission spectra as a function of the light propagation distance, i.e. the distance z travelled by light from the fiber excitation point to the spectrometer. Fig. 13 shows the emission spectra obtained when LY10LR0 (top-left side), LY5LR5 (top-right side) and LY0LR10 (bottom-left side) samples are excited at different launching points, varying the light-propagation distance along the fibers. The blue-colored spectra were taken close to the detector and the greenish ones were obtained further away. From the closest (as close as the SMA connector made possible) to the farthest, the difference in propagation distance is 85 mm. For all the samples, when the excitation point is moved farther from the detector, the amount of measured emitted intensity is reduced and the emission peak is shifted toward longer wavelengths, as expected. However, the observed shifts are slighter than those observed for POFs doped with other organic molecules, such as rhodamine dyes or conjugated polymers, which is a direct consequence of the minor overlap between the corresponding absorption and emission spectra of the Lumogen dyes [6].

On the other hand, taking into account the reduction on the emission intensity for the propagation distance considered, LY10LR0 and LY0LR10 samples follow a similar behavior, losing 35 % and 40 % of their initial intensity, respectively. In the case of sample LY5LR5,

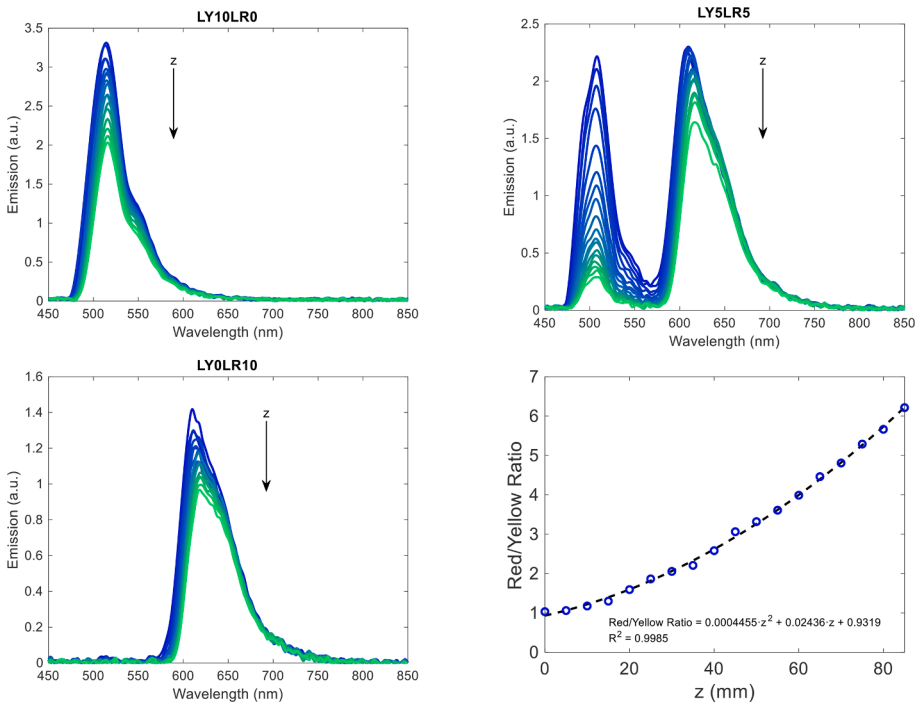

Fig. 13. Emission spectra as a function of light propagation distance (z) for LY10LR0 (top-left side), LY5LR5 (top-right side) and LY0LR10 (bottom-left side) fiber samples excited at 445 nm by side-illumination technique. The increase in propagation distance is 85 mm, represented with bluish colors those spectra measured closest to the detector and with greenish colors those furthest away. Bottom-right side: Ratio between the maximum emission intensities corresponding to Lumogen Red and to Lumogen Yellow as a function of the propagation distance for the LY5LR5 sample. The point of the fiber closest to the detector was set to zero.

although the reduction observed in the red emission band is similar to the other two samples, 30 %, the reduction observed in the green emission band rises to 90 %. This can be explained as follows. For short fiber distances, the novel ring-doped structure of our samples makes it possible for a part of the emission corresponding to Lumogen Yellow propagate, through the central part of the fiber, without any iteration with Lumogen Red molecules. Meanwhile, the other part of the emission interacts, providing the coexistence of both emission bands. However, as the propagation distance increases, there is a greater likelihood of interactions, promoting reabsorption effects. Moreover, it is worth mentioning that the emission intensity of the LY5LR5 sample is higher than that corresponding to the LY0LR10 sample, due to the energy transfer process between dopants. These observed emission features as a function of the propagation distance could be very useful to achieve tuning characteristic in the emission of light sources based on these active POFs. As the side-illumination technique is employed to excite the fibers, the excitation point and consequently, the propagation distance, can be easily adjusted and modified depending on the application, without any need of changing the POF.

The bottom-right side of Fig. 13 shows the ratio between the maximum emission intensities corresponding to Lumogen Red and to Lumogen Yellow as a function of the propagation distance for the LY5LR5 sample. The evolution is quadratic with a good value of coefficient of determination, 0.9985. This fact could be very interesting to accurately detect the incident point of the excitation, which is directly related to the light propagation distance, and consequently make a position or displacement sensor.

The attenuation of the doped POFs can also be obtained from the analysis of the light propagation distance. Assuming that the illuminated fiber section behaves as a plane-wave source, the light irradiance propagating towards the spectrometer at any wavelength λ decays exponentially with the propagation distance z as follows [27,28]:

$$I(\lambda, z) = I_0(\lambda)\exp[-\alpha(\lambda)\cdot z] \quad (1)$$

where $I_0(\lambda)$ represents the light irradiance measured at $z = 0$ at the wavelength λ, and $\alpha(\lambda)$ is the linear attenuation coefficient at the considered wavelength. Fig. 14 shows the linear-attenuation coefficients calculated for LY10LR0, LY5LR5 and LY0LR10 fiber samples by fitting

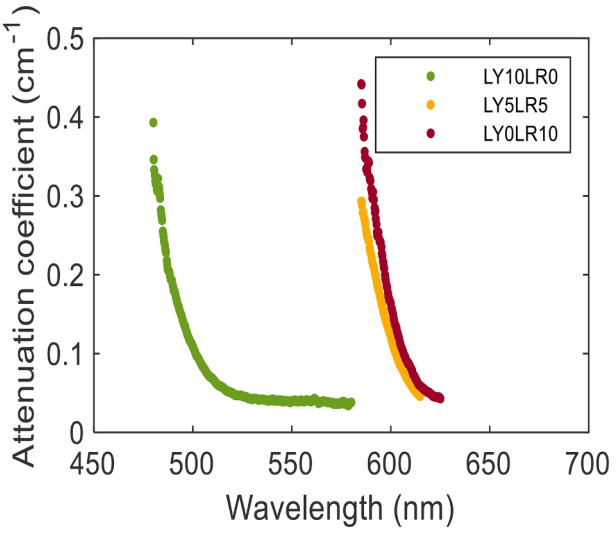

Fig. 14. Linear attenuation coefficients of LY10LR0, LY5LR5 and LY0LR10 fiber samples excited at 445 nm by side-illumination technique.

the experimental data to Equation (1) for several wavelengths. The main reason for the possible increase in attenuation during the doping process stems from the excess plasticization and relaxation of the polymer molecules by small solvent molecules, so that the microstructure inside the POFs is permanently modified. However, the attenuation values obtained are very similar to those reported in the literature for other doped PMMA POFs [22] and also for POFs doped with Lumogen dyes but fabricated by more conventional fabrication techniques, such as the thermal fiber-drawing technique [5]. This implies that the doping procedure employed in this work did not add extra losses to the fibers.

For a better understanding of the energy transfer process from Lumogen Yellow to Lumogen Red, the fluorescence decay profiles of all doped POFs were recorded -excited at 445 nm by the side-illumination technique-, as it is shown in Fig. 3. The top side of Fig. 15 represents the time-resolved decay profiles obtained integrating the spectral range

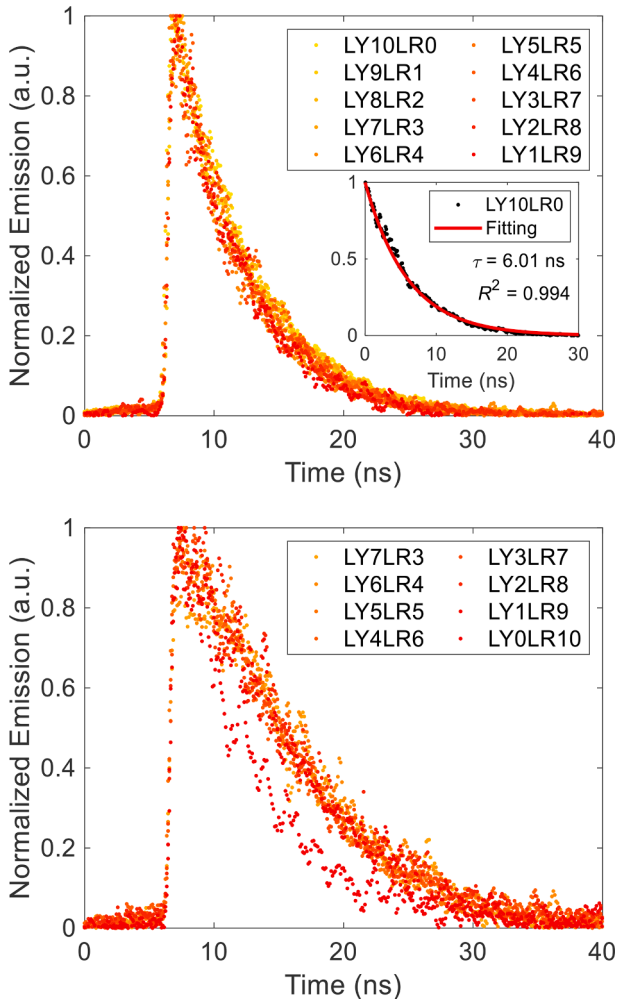

Fig. 15. Time-resolved decay profiles for those doped POFs in which (top) the Lumogen Yellow and/or (bottom) Lumogen Red are presented. The inset on top side of the figure shows the exponential fitting of the emission of the sample LY10LR0 to Equation (2) and the calculated values (fluorescence lifetime and the coefficient of determination).

460 nm-570 nm for those doped POFs in which the Lumogen Yellow is present. As already known, the fluorescence decay of a dopant can be expressed as [34]:

$$I(t) = I_0 \exp(-t/\tau) \tag{2}$$

where, I_0 is the intensity at time zero (upon excitation) and τ is the lifetime. The inset on the top side of Fig. 15 shows the exponential fitting of the emission of the LY10LR0 sample to Equation (2), as well as the obtained lifetime value for the Lumogen Yellow τ_{LY} and its coefficient of determination. The same process was repeated for the rest of the curves represented in the figure to calculate all the lifetimes. For the curves shown in the bottom side of Fig. 15, the lifetime values for the Lumogen Red τ_{LR} were obtained, integrating the spectral range 570 nm-800 nm and repeating, in the same way, the fitting process. All calculated values, shown in Table 1, are similar, with lifetimes in the 5–10 ns time range, which is in good agreement with values previously reported for organic fluorophores [35,36]. By using these lifetime values, the non-radiative energy transfer efficiency ($\eta_{LY\rightarrow LR}$) from Lumogen Yellow to Lumogen Red were estimated [37]:

$$\eta_{LY\rightarrow LR} = 1 - \frac{\tau_{LY}(\text{co-doped})}{\tau_{LY}(\text{LY10LR0})} \tag{3}$$

$\tau_{LY}(\text{co-doped})$ and $\tau_{LY}(\text{LY10LR0})$ are the lifetimes of Lumogen Yellow in the presence and absence of Lumogen Red, respectively. Based on this equation, the efficiency values were calculated and listed also in Table 1.

Table 1
Fluorescence lifetimes and energy transfer efficiencies for our doped POFs.

Sample	τ_{LY}(ns) and R^2	τ_{LR}(ns) and R^2	$\eta_{LY\rightarrow LR}$
LY10 LR0	6.01 0.994		
LY9 LR1	5.65 0.996		0.060
LY8 LR2	5.68 0.993		0.055
LY7 LR3	5.34 0.992	8.76 0.973	0.111
LY6 LR4	5.01 0.991	9.56 0.974	0.166
LY5 LR5	5.15 0.993	8.98 0.979	0.143
LY4 LR6	5.37 0.989	9.01 0.975	0.106
LY3 LR7	5.36 0.986	9.13 0.980	0.108
LY2 LR8	5.13 0.992	8.85 0.976	0.146
LY1 LR9	5.01 0.987	9.11 0.965	0.166
LY0 LR10		6.21 0.985	

It is noticeable that τ_{LY} are shorter and τ_{LR} are larger for co-doped samples, which means that there is a non-radiative energy transfer process from Lumogen Yellow to Lumogen Red [29]. The absence of τ_{LR} values for samples LY9LR1 and LY8LR2 is a consequence of undetectable signal values in the corresponding spectral range and it can be explained looking at their energy transfer efficiency values, since they have the lowest values. The rest of the co-doped samples present quite similar lifetime values and with efficiencies ranging from 10 % to 16 %. Even though the sample LY5LR5 is not the most efficient, having a slightly lower value than the LY6LR4 and LY1LR9 samples, it has the best emission properties, with good intensity values and broad tuning characteristics, as demonstrated during the paper. All these features, together with the other optical properties observed throughout the paper, are very important when designing FOP-based light sources and sensors.

4. Conclusions

This paper shows a method to fabricate active POFs with a novel ring-doped structure by using the solution-doping technique. One of the advantages of this doping technique is the ease of controlling the amount of dopant penetration because of the clear boundary between the doped outer ring and the intact inner region. In addition, the technique allows doping only one end of the fiber, which makes it possible to create fibers that are active and passive at the same time, without the need to connect fibers of different nature to each other and thus avoiding coupling losses. Specifically, two perylene derivatives were chosen, i.e. Lumogen Yellow 083 and Lumogen Red 305, with a large overlap between the emission band of the former and the absorption band of the latter. Then, active POFs doped with each of them, and with their combinations, were fabricated achieving in each case a dopant penetration of 35 %. Their spectral characteristics and the evolution of the emission intensities were measured and analyzed as functions of the dopant combination, the pumping power and wavelength, and the light propagation distance. The results obtained show that these doped fibers have a great versatility in emission depending on these parameters. Moreover, it was also concluded that higher emission intensities could be achieved in the red emission band using both dopants together instead of using only Lumogen Red, it is because of the energy transfer between dopants. Finally, a time-resolved characterization of the doped POFs was also carried out to measure their fluorescence lifetimes and to extract information about the energy transfer from Lumogen Yellow to Lumogen Red. These optical features and ease of fabrication could be very interesting in the design process of all-optical devices based on active POFs, such as broadband or dual-band light sources and sensors. In addition, these fibers are also expected to have interesting properties as luminescent solar concentrators, which will be the subject of research in future work.

CRediT authorship contribution statement

Igor Ayesta: Conceptualization, Methodology, Investigation, Writing – original draft, Data curation. **Mikel Azkune:** Conceptualization, Methodology, Investigation, Writing – original draft, Data curation. **María Asunción Illarramendi:** Conceptualization, Investigation, Writing – original draft. **Eneko Arrospide:** Investigation. **Joseba Zubia:** Investigation, Funding acquisition. **Gaizka Durana:** Funding acquisition, Investigation.

Declaration of Competing Interest

The authors declare that they have no known competing financial interests or personal relationships that could have appeared to influence the work reported in this paper.

Data availability

Data will be made available on request.

Acknowledgements

These results are funded in part by the Ministerio de Ciencia e Innovación -under projects RTC2019-007194-4, PID2021-122505OB-C31 and TED2021-129959B-C21,- and in part by Gobierno Vasco/Eusko Jaurlaritza under projects IT1452-22 and ELKARTEK (KK-2021/00082, KK-2021/00092).

References

[1] K. Jakubowski, C.-S. Huang, L.F. Boesel, R. Hufenus, M. Heuberger, Recent advances in photoluminescent polymer optical fibers, Curr. Opin. Solid State Mater. Sci. 25 (2021), 100912, https://doi.org/10.1016/j.cossms.2021.100912.
[2] Y. Koike, Fundamentals of Plastic Optical Fibers, Wiley-VCH, Weinheim, Germany, 2015.
[3] C.-A. Bunge, M. Beckers, T. Gries, Polymer Optical Fibres. Fibre Types, Materials, Fabrication, Characterisation and Applications, Woodhead Publishing, Duxford, United Kingdom, 2017.
[4] P. Moraitis, R.E.I. Schropp, W.G.J.H.M. van Sark, Nanoparticles for Luminescent Solar Concentrators - A review, Opt. Mater. 84 (2018) 636–645, https://doi.org/10.1016/j.optmat.2018.07.034.
[5] I. Parola, E. Arrospide, F. Recart, M.A. Illarramendi, G. Durana, N. Guarrotxena, O. García, J. Zubia, Fabrication and characterization of polymer optical fibers doped with perylene-derivatives for fluorescent lighting applications, Fibers 5 (2017), https://doi.org/10.3390/fib5030028.
[6] I. Ayesta, M.A. Illarramendi, J. Arrue, F. Jiménez, J. Zubia, I. Bikandi, J. M. Ugartemendia, J.-R. Sarasua, Luminescence Study of Polymer Optical Fibers Doped With Conjugated Polymers, J. Lightwave Technol. 30 (2012) 3367–3375, https://doi.org/10.1109/JLT.2012.2218216.
[7] C. Hirose, S. Kamimura, R. Furukawa, Waveguide optimization and its evaluation of a doped polymer optical fiber designed for visual detection of stress, Jpn. J. Appl. Phys. 59 (2020), https://doi.org/10.7567/1347-4065/ab591e.
[8] X. Lu, K. Hicke, M. Breithaupt, C. Strangfeld, Distributed Humidity Sensing in Concrete Based on Polymer Optical Fiber, Polymers 13 (2021), https://doi.org/10.3390/polym13213755.
[9] J. Arrue, A. Vieira, B. García-Ramiro, F. Jiménez, M.A. Illarramendi, J. Zubia, Modelling of polymer optical fiber-based solar concentrators, Method. Appl. Fluoresc. 9 (2021), https://doi.org/10.1088/2050-6120/abfa6d.
[10] J. Grandes, M.A. Illarramendi, E. Arrospide, I. Bikandi, I. Aramburu, N. Guarrotxena, O. García, J. Zubia, Temperature effects on the emission of polymer optical fibers doped with Lumogen dyes, Opt. Fiber Technol. 72 (2022), https://doi.org/10.1016/j.yofte.2022.102980.
[11] J. He, W.-K.-E. Chan, X. Cheng, M.-L.-V. Tse, C. Lu, P.-K.-A. Wai, S. Savovic, H.-Y. Tam, Experimental and theoretical investigation of the polymer optical fiber random laser with resonant feedback, Adv. Opt. Mater. 6 (2018), https://doi.org/10.1002/adom.201701187.
[12] I. Parola, M.A. Illarramendi, J. Arrue, A. Tagaya, Y. Koike, Characterization of the optical gain in doped polymer optical fibres, J. Lumin. 177 (2016) 1–8, https://doi.org/10.1016/j.jlumin.2016.04.009.
[13] D. Sáez-Rodríguez, K. Nielsen, H.K. Rasmussen, O. Bang, D.J. Webb, Highly photosensitive polymethyl methacrylate microstructured polymer optical fiber with doped core, Opt. Lett. 38 (2013), https://doi.org/10.1364/OL.38.003769.
[14] T. Wang, Q. Wang, Y. Luo, W. Qiu, G.-D. Peng, B. Zhu, Z. Hu, G. Zou, Q. Zhang, Enhancing photosensitivity in near UV/vis band by doping 9-vinylanthracene in polymer optical fiber, Opt. Commun. 307 (2013) 5–8, https://doi.org/10.1016/j.optcom.2013.06.001.
[15] E. Arrospide, I. Bikandi, I. García, G. Durana, G. Aldabaldetreku, J. Zubia, Mechanical properties of polymer-optical fibres, in: C.-.-A. Bunge, T. Gries, M. Beckers (Eds.), Polymer Optical Fibres, Woodhead Publishing, Duxford, United Kingdom, 2017, pp. 201–216.
[16] E. Arrospide, M.A. Illarramendi, I. Ayesta, J. Zubia, G. Durana, Effects of fabrication methods on the performance of luminescent solar concentrators based on doped polymer optical fibers, Polymers 13 (2021) 1–15, https://doi.org/10.3390/polym13030424.
[17] M. Mignanelli, K. Wani, J. Ballato, S. Foulger, P. Brown, Polymer microstructured fibers by one-step extrusion, Opt. Express 15 (2007) 6183–6189, https://doi.org/10.1364/OE.15.006183.
[18] R. Hirose, M. Asai, A. Kondo, Y. Koike, Preparation of graded-index plastic optical fiber by co-extrusion process, Proc. SPIE 6470, Organic Photonic Materials and Devices IX (2007), 64700K. 10.1117/12.700193.
[19] W. Ding, J. Sun, G. Chen, L. Zhou, J. Wang, X. Gu, J. Wan, X. Pu, B. Tang, Z. l. Wang, Stretchable multi-luminescent fibers with AIEgens, J. Mater. Chem. C 7 (2019) 10769–10776, https://doi.org/10.1039/C9TC03461G.
[20] Y. He, E. Du, X. Zhou, J. Zhou, Y. He, Y. Ye, J. Wang, B. Tang, X. Wang, Wet-spinning of fluorescent fibers based on gold nanoclusters-loaded alginate for sensing of heavy metal ions and anti-counterfeiting, Spectrochim, Acta Part A Mol. Biomol. Spectrosc. 230 (2020) 1–10, https://doi.org/10.1016/j.saa.2020.118031.
[21] P. Stajanca, I. Topolniak, S. Pötschke, K. Krebber, Solution-mediated cladding doping of commercial polymer optical fibers, Opt. Fiber Technol. 41 (2018) 227–234, https://doi.org/10.1016/j.yofte.2018.02.008.
[22] I. Ayesta, M. Azkune, E. Arrospide, J. Arrue, M. Illarramendi, G. Durana, J. Zubia, Fabrication of active polymer optical fibers by solution doping and their characterization, Polymers 11 (2018), https://doi.org/10.3390/polym11010052.
[23] C. Tian, C. Ma, X. Han, Z.F. Zhang, Doping of polymer optical fiber cladding by Rhodamine 6G in aqueous solution at elevated temperature, Polym. Bull. (2022), https://doi.org/10.1007/s00289-022-04224-z.
[24] M.C.J. Large, S. Ponrathnam, A. Argyros, N.S. Pujari, F. Cox, Solution doping of microstructured polymer optical fibres, Opt. Express 12 (2004), https://doi.org/10.1364/OPEX.12.001966.
[25] Z.F. Zhang, F. Ye, X. Ma, W. Zhao, H. Wang, Accelerated doping of trans-4-stilbenemethanol into polymer optical fibers by binary non-solvent/solvent mixtures, Opt. Fiber Technol. 58 (2020), https://doi.org/10.1016/j.yofte.2020.102265.
[26] E. Arrospide, G. Durana, M. Azkune, G. Aldabaldetreku, I. Bikandi, L. Ruiz-Rubio, J. Zubia, Polymers beyond standard optical fibres – fabrication of microstructured polymer optical fibres, Polym. Int. 67 (2018) 1155–1163, https://doi.org/10.1002/pi.5602.
[27] R. Kruhlak, M. Kuzyk, Side-illumination fluorescence spectroscopy. I. principles, J. Opt. Soc. Am. 16 (1999) 1749–1755, https://doi.org/10.1364/JOSAB.16.001749.
[28] R. Kruhlak, M. Kuzyk, Side-illumination fluorescence spectroscopy. II. Applications to squaraine-dye-doped polymer optical fibers, J. Opt. Soc. Am. 16 (1999) 1756–1767, https://doi.org/10.1364/JOSAB.16.001756.
[29] G. Saavedra-Rodriguez, U. Pal, R. Sánchez-Zeferino, M.E. Álvarez-Ramos, Tunable White-Light Emission of Co2+ and Mn2+ Co-Doped ZnS Nanoparticles by Energy Transfer between Dopant Ions, J. Phys. Chem. C 124 (2020) 3857–3866, https://doi.org/10.1021/acs.jpcc.9b10890.
[30] M.A. Illarramendi, J. Zubia, L. Bazzana, G. Durana, G. Aldabaldetreku, J. R. Sarasua, Spectroscopic Characterization of Plastic Optical Fibers Doped With Fluorene Oligomers, J. Lightwave Technol. 27 (2009) 3220–3226, https://doi.org/10.1109/JLT.2008.2010274.
[31] P. Miluski, M. Kochanowicz, J. Żmojda, A. Baranowska, T. Ragiń, D. Dorosz, White light emission PMMA fibre co-doped with 1,4-Bis(2-methylstyryl) benzene and Rhodamine B for new optical applications, Ceram. Int. 46 (2020), https://doi.org/10.1016/j.ceramint.2020.03.227.
[32] L. Persano, A. Camposeo, D. Pisignano, Active polymer nanofibers for photonics, electronics, energy generation and micromechanics, Prog. Polym. Sci. 43 (2015) 48–95, https://doi.org/10.1016/j.progpolymsci.2014.10.001.
[33] M. Enculescu, A. Evanghelidis, I. Enculescu, White-Light Emission of Dye-Doped Polymer Submicronic Fibers Produced by Electrospinning, Polymers 10 (2018), https://doi.org/10.3390/polym10070737.
[34] C. Albrecht, J.R. Lakowicz, Principles of fluorescence spectroscopy, Anal. Bioanal. Chem. 390 (2008) 1223–1224, https://doi.org/10.1007/s00216-007-1822-x.
[35] C. Papucci, R. Charaf, C. Coppola, A. Sinicropi, M. di Donato, M. Taddei, P. Foggi, A. Battisti, B. de Jong, L. Zani, A. Mordini, A. Pucci, M. Calamante, G. Reginato, Luminescent solar concentrators with outstanding optical properties by employment of D-A–D quinoxaline fluorophores, J. Mater. Chem. C 9 (2021) 15608–15621, https://doi.org/10.1039/D1TC02923A.
[36] R. Reisfeld, V. Levchenko, T.S. Saraidarov, E. Rysiakiewicz-Pasek, M. Baranowski, A. Podhorodecki, J. Misiewicz, T. Antropova, Steady state and femtosecond spectroscopy of Perylimide Red dye in porous and sol–gel glasses, Chem. Phys. Lett. 546 (2012) 171–175, https://doi.org/10.1016/j.cplett.2012.07.073.
[37] W. Sun, H. Li, B. Li, Energy transfer and luminescence properties of a green-to-red color tunable phosphor Sr8MgY(PO4)7: Tb3 +, Eu3+, J. Mater. Sci. Mater. Electron. 30 (2019) 9421–9428, https://doi.org/10.1007/s10854-019-01272-6.